Separation and Purification Technology 227 (2019) 115711

Contents lists available at ScienceDirect

Separation and Purification Technology

journal homepage: www.elsevier.com/locate/seppur

Effect of the addition of precipitated ferric chloride on the morphology and settling characteristics of activated sludge flocs

E. Asensi[a], D. Zambrano[b,*], E. Alemany[c], D. Aguado[a]

[a] CALAGUA – Unidad Mixta UV-UPV, Institut Universitari d'Investigació d'Enginyeria de l'Aigua i Medi Ambient – IIAMA, Universitat Politècnica de València, Camí de Vera s/n, 46022 Valencia, Spain

[b] Department of Chemical Engineering and Environmental Technologies – Catalysis, Molecular Separations and Reactor Engineering Group (CREG) – Aragón Institute of Engineering Research (I3A) – Universidad Zaragoza, Mariano Esquillor s/n, 50018 Zaragoza, Spain

[c] Departamento de Matemática Aplicada, Universitat Politècnica de València, Camí de Vera s/n, 46022 Valencia, Spain

ARTICLE INFO

Keywords:
Activated sludge
Floc morphology
Image analysis
Optical monitoring
Settling velocity

ABSTRACT

The activated sludge process is the most widely used biological wastewater treatment process. For a successful operation of this aerobic suspended growth process, the microorganisms must aggregate to form flocs that settle in the secondary settler. Poor plant operation or the increasingly stringent effluent quality requirements may lead in existing WWTPs to a failure to meet the effluent discharge legal requirements. A technically viable solution to this problem is to improve the suspended solid removal at the secondary settler. A low-cost option for short periods (eg., disturbances or emergency situations) would be to improve the settling properties of the sludge, via the addition of coagulants or ballasted sedimentation. The solid-liquid separation in the secondary settler is affected by the density, size and other characteristics of the flocs. For this reason, in this work, a fully automatic toolbox for recognizing activated sludge flocs and performing their morphological characterization based on digital image analysis and statistical processing was developed. This characterization included the determination of the equivalent diameter of the flocs, their area, perimeter, length and width, radius of gyration, reduced gyration radius, aspect ratio, form factor, roundness and fractal dimensions. The toolbox was used to characterize the activated sludge flocs from a full-scale urban WWTP, as well as the observed changes in their characteristics due to the addition of a dose of precipitated ferric chloride. A new methodology based on geometric properties (aspect ratio and floc size distribution) is proposed to discriminate the debris from small activated sludge flocs. The addition of the precipitate and the subsequent flocculation process produced larger flocs with more area and less perimeter, that is, larger, more compact, closed and regular flocs. The size and density of the flocs, as well as the hindered settling velocity, linearly increased with the addition of precipitated ferric chloride. Partial least squares (PLS) regression of all collected data revealed that the volumetric fraction of the sludge, the suspended solid concentration and the fractal dimension that relates area – perimeter were the variables most correlated with the hindered settling velocity.

Nomenclature

SS	suspended solids (g L^{-1})
nVSS	non-volatile suspended solids (g L^{-1})
Δ_nVSS	increment of non-volatile suspended solids (g L^{-1})
ρ_f	floc density (g mL^{-1})
ρ_s	dry sludge density (g mL^{-1})
Fv	volumetric fraction, $Fv = \frac{SS}{\rho_s}$
d	dose of ferric chloride precipitate (mL L^{-1})
ε_X	standard error of variable X
L	floc length (μm), Length of the major axis of the ellipse having the same normalized second central moments as the region comprised by the floc
W	floc width (μm), Length of the minor axis of the ellipse having the same normalized second central moments as the region comprised by the floc
P	floc perimeter (μm)
A	projected floc area (μm^2)
D_{eq}	equivalent diameter (μm), $D_{eq} = 2\sqrt{\frac{A}{\pi}}$
r_G	radius of gyration (μm), $r_G = \sqrt{\frac{1}{N}\sum_{i=1}^{N} d_i^2}$, d_i: distance from each pixel to centre of masses
RGR	reduced gyration radius, $RGR = \frac{2r_G}{D_{eq}}$
AR	aspect ratio, $AR=1+\frac{4}{\pi}\left(\frac{L}{W}-1\right)$

* Corresponding author.
E-mail address: dzjuca@unizar.es (D. Zambrano).

https://doi.org/10.1016/j.seppur.2019.115711
Received 5 December 2018; Received in revised form 14 June 2019; Accepted 17 June 2019
Available online 18 June 2019
1383-5866/

FF	form factor, $FF = \frac{4\pi A}{P^2}$
R	roundness, $R = \frac{4A}{\pi L^2}$
$Df_{P\text{-}L}$	fractal dimension relating perimeter to length, $P \propto L^{Df_{P-L}}$
$Df_{A\text{-}L}$	fractal dimension relating area to length, $A \propto L^{Df_{A-L}}$
$Df_{A\text{-}P}$	fractal dimension relating area to perimeter, $A \propto P^{2/Df_{A-P}}$
%Nb*	percentage of flocs number
%Area*	percentage of flocs area
Vs	hindered settling velocity (cm min^{-1})
Vs_i	hindered settling velocity with no added precipitate (cm min^{-1})
Abbreviations	
WWTP	waste water treatment plant
PCA	principal component analysis
PLS	partial least squares

*Determined for small ($D_{eq} < 25\,\mu m$), intermediate ($25\,\mu m < D_{eq} < 250\,\mu m$), and large ($D_{eq} > 250\,\mu m$) flocs.

1. Introduction

The rising concern about the protection of the environment and the increasingly stringent effluent quality requirements imposed by law, have led to a large number of wastewater treatment plants (WWTPs) equipped with processes for nutrient removal. Most WWTPs implement the activated sludge process as a biological wastewater treatment stage for carbon and nutrient removal [1]. In this aerobic suspended growth process, wastewater pollutants are used by the microorganisms as substrate for their growth [2]. The formed biomass aggregates in sludge flocs. The characteristics of these sludge flocs (size, density, form, …) determine the efficiency of the solid-liquid separation process at the secondary settler, and therefore can definitely impact on the quality of the effluent.

Improving the suspended solid removal in the secondary settler is an option when the WWTP effluent discharge requirements are demanding and cannot be achieved via biological nutrient removal and/or chemical precipitation. The use of sand filters or membranes as tertiary treatment are structural solutions that require significant investment cost and construction time. An alternative option for short periods (eg., disturbances or emergency situations) that does not require high investment costs would be to improve the sedimentation characteristics of the activated sludge. This can be achieved by the addition of an inert compound (sand, kaolin, etc.), practice known as “ballasted sedimentation” [3–6]. The addition of the inert compound improves the sludge sedimentability and reduces the non-sedimentable solids due to absorption by the flocs and to “entrainment” of the compound. Moreover, if an iron precipitate is added, not only the phosphorus contained in the suspended solids is removed but also part of the soluble phosphorus can be removed through absorption [7–9].

The morphological properties of the flocs have significant influence on the settleability of activated sludge in full-scale wastewater treatment processes [10–13]. Changes in the sludge flocs characteristics can be due to process disturbances like entry of toxic compound [14] or bulking events [15], as well as to changes in operational conditions [16]. This disturbances can also affect the sludge sedimentability [15,17]. For monitoring activated sludge processes and early detection of problems, quantitative image analysis has proven to be highly useful and valuable [18,19]. For better process understanding, different researches have explored the effect of coagulants and different ballasting materials on the floc structure [6,20,21]. However, none of these studies has focused on the effect of the addition of precipitated ferric chloride on the morphology and settling characteristics of the activated sludge flocs. For this purpose, in this work, a fully automatic toolbox for recognizing activated sludge flocs and performing their morphological characterization based on digital image analysis and statistical processing was developed. This toolbox was used to characterize the activated sludge flocs from a full-scale urban WWTP, and the changes in their characteristics due to the addition of a dose of precipitated ferric chloride. A precipitated reagent neutralized at pH 7 was selected to avoid affecting the pH of the biological process when implementing the process in the full-scale WWTP. This precipitate can favour flocs' formation and contribute to the removal of soluble phosphorus via absorption and to the increase of the settling velocity.

Table 1
Precipitated ferric chloride dose (d) in each test.

Sludge sample	Number of tests	d [mL L^{-1}]					
S1	4	0	2.5	10	15		
S2	4	0	1.25	6.25	8.5		
S3	5	0	2.5	5	10	15	
S4	6	0	2.5	5	10	12.5	15

2. Materials and methods

2.1. Experimental procedure

A total of 19 tests were performed to study the influence of the addition of precipitated ferric chloride on the morphology and settling characteristics of the sludge. Sludge samples were collected from Carraixet WWTP (Valencia, Spain) at four different days. In each test, a precise volume in the range 0–15 mL of precipitated ferric chloride was added (see Table 1).

The precipitated ferric chloride solution was prepared with a concentration of 24 g Fe L^{-1} using ferric chloride *hexa*-hydrated $FeCl_36H_2O$ (molecular weight 270.30 g mol^{-1} and 98% purity) dissolved in deionized water while the pH was monitored, and a NaOH (10 N) solution that was progressively added until the pH was 7. This pH value was selected to avoid affecting the pH of the biological process when implementing the reagent dosing in the WWTP.

The tests were performed on a program-controlled jar-test apparatus with 1 L of sludge. The desired dosage of precipitated ferric chloride solution was added at the beginning of the mixing. In the jar-test apparatus, the following stages were implemented: rapid stirring at 120 rpm for 10 min followed by slow stirring at 25 rpm for 20 min. After finishing the slow stirring, the sludge was used for optical microscopy characterization of the flocs, for density and suspended solid determination, and in the settling tests that were conducted to determine the hindered settling velocity.

The duration of the rapid mixing was chosen to eliminate the possible memory effect of the sludge in the sedimentation process [22,23]. According to François *et al.* [24], the initial rapid stirring of the activated sludge allows reproducing the hydrodynamic conditions of the treatment plant where the sludge experiences high turbulences due to the action of aerators in the biological reactor and the pumping of sludge. Later, the activated sludge experiences hydraulic flocculation at the entry of the secondary settler in the treatment plant, where it flows through the energy-dissipating inlet and the feed well.

2.2. Image analysis protocol

Image analysis techniques were used to determine the distribution of the activated sludge floc size (equivalent diameter, length, area, perimeter, radius of gyration), fractal dimensions and morphological parameters (reduced gyration radius, aspect ratio, form factor, roundness). The fractal dimension is an extension and generalization of the Euclidean dimension that reflects the complexity and irregularities of a given structure. Three fractal dimensions were calculated, since the volume of flocs was not measured. Using image analysis techniques, the projected area, length and perimeter was measured. This information was used to create log – log plots for which the slope of the linear regression line corresponds to the value of the fractal dimension. All the key quantitative parameters were calculated as defined in [18] and are included in nomenclature list.

Fig. 1. Main steps in the processing of the images obtained with the microscope.

A volume of 65 µL of sludge sample was taken to a slide and covered with a 24 × 36 mm cover slip for image acquisition in bright field microscopy. Images were acquired using a Hund Wetzlar H500 microscope with 50x magnification (and 100x for the debris characterization), coupled to a VisiCam 10.0 camera (3856 × 2764 pixels). The microscope magnification used allowed to capture the full size range of the flocs, thus, leading to representative results. In this work, large flocs were produced as a result of the precipitated addition and thus the use of a higher magnification was observed to cut most of the largest flocs.

To obtain a sample of images large enough to perform a statistical analysis, a minimum of 121 images (3x40 images per slide plus one background image) were taken from each test. The images were processed using an application program developed in MATLAB (MathWorks®), following the methodology introduced by Mesquita *et al.* [25]. A summary of the processing steps is given in Fig. 1. The same application was recently used in [23].

Image pre-processing and segmentation comprised several operations performed on the original images, which included: (a) background image pre-processing, consisting on a correction of the background image in order to enhance pixels corresponding to noise caused by light variation, enhancement achieved by subtraction of the background image from the original image; (b) automatic transformation to a graylevel image; (c) elimination of noise pixels caused by light variation using the frequency histogram and automatic determination of optimal threshold level; (d) intensity adjustment, to reduce the overall brightness of the image and too increase the contrast in the brightest areas; (e) elimination of noise in the foreground image by morphological operations (erosion and reconstruction).

The image segmentation allowed the detection of the external and internal (pores) edges of the sludge flocs in a large number of images processed sequentially. Flocs in each image were identified as objects on a background. Visual inspection, made by overlapping the final image to the original one (see Fig. 2), allowed verifying that image processing was performed correctly.

Finally, the statistical analysis of the quantitative parameters, measured on the detected flocs in the image, was performed. This analysis included for each measured parameter the determination of the basic descriptive statistics (to assess center, dispersion, skewness and kurtosis of the data set), histogram plotting, distribution fitting, outlier detection and ANOVA or Krustal-Wallis tests to assess statistically significant differences in central values when compared to the values obtained from samples with an added dose of precipitated $FeCl_3$.

Incomplete flocs lying at the edges of the image and particles classified as debris were removed prior to the statistical analysis. Some organisms, such as rotifers, and other non sludge flocs objects were identified from the outliers of the statistical analysis using both, the morphological parameters and Chebyshev's intervals, and were removed before performing the final statistical determination of the quantitative parameters of interest on the activated sludge flocs. Outlier from data was detected using the Chebyshev outlier detection method based on Chebyshev inequality. Three parameters were used (porosity, AR and RGR) with a 98% Chebyshev's confidence intervals. The remaining morphological parameters (R and FF) did not provide useful information to this purpose (i.e., detection of non-sludge floc objects).

Finally, to determine the probability distributions of the data, for each size and morphological parameter a probability test on probabilistic paper was performed. The following theoretical distributions were considered in this process: normal, lognormal, Weibull, exponential and Rayleigh.

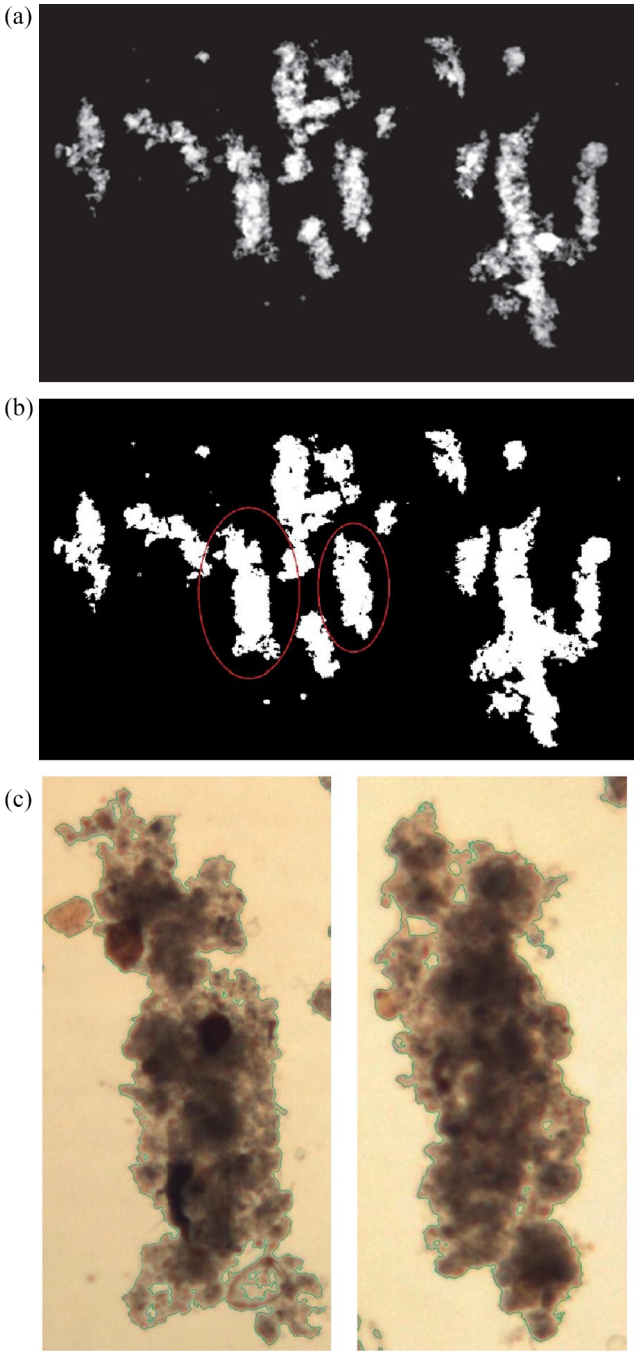

Fig. 2. Visual inspection at different processing stages: (a) Image pre-processed (b) Image segmented (red circles point out the flocs shown in figure c) (c) visual verification of the segmentation algorithm results.

2.3. Settling tests

Hindered settling tests were performed as described in [26] using one-liter glass graduated cylinder. The dilution of the sludge was performed using supernatant from the secondary settler. The interface height in the settling test was calculated as a time dependent function. No stirring of sludge was performed during the test so as not to interfere

with possible floc aggregation [22].

To evaluate the effect of the addition of precipitated ferric chloride, settling tests were carried out in the 19 tests described in the experimental procedure, considering samples without and samples with different doses of precipitated $FeCl_3$.

2.4. Analytical methods

The concentration of suspended solids (SS), volatile suspended solids (VSS), non-volatile suspended solids (nVSS), phosphates and iron were determined according to the Standard Methods [26].

A pycnometer method [27] was used to determine the density of the dry sludge (ρ_s) while the floc density (ρ_f) was determined with a method based on centrifugation in homogenous density solutions [28]. This method was chosen because it is a widely accepted and validated method for activated sludge and allows quantifying the density distribution. Moreover, it is an easy and direct method that does not requires a specialized laboratory equipment. The method is based on the centrifugation of the activated sludge in different Percoll homogeneous density solutions. For a particular Percoll homogeneous density solution, the activated sludge fraction in the upper and lower part of the tube test is determined. Depending of the flocs' density with respect to the Percoll solution, those with higher density will be at the bottom of the tube test, while the flocs with lower density will be in the upper part. Later, considering the results from all solutions, the histogram of the density distribution of the flocs is plotted and the mean and standard deviation obtained from the fitted normal distribution.

2.5. Mathematical and statistical methods

MATLAB (MathWorks®) was used to develop the image processing software which included numerical calculus and statistical analysis. Most of the graphics in the manuscript were elaborated and laid out in Excel. SIMCA-P 10.0 software (Umetrics, Umea, Sweden) was used for the multivariate analysis.

3. Results and discussion

3.1. Density and concentration of the activated sludge

Table 2 shows the concentration of SS and nVSS in each test. A dry sludge density (ρ_s) of $1.524 \pm 0.015\ g\ mL^{-1}$ and a floc density (ρ_f) of $1.035 \pm 0.004\ g\ mL^{-1}$ were obtained from samples with no precipitate added. To visualize the effect of the addition of precipitate, the observed variables can be represented in terms of the added precipitate, expressed as an increment of non-volatile suspended solids (Δ _nVSS) with respect to the concentration of nVSS found in the test with no added precipitate (i.e., Δ _nVSS = [nVSS − nVSSi]).

The precipitate dose (d) used ranged from 0 to 15 mL L^{-1}, which is equivalent to a dose between 0 and 360 mg Fe L^{-1}. Considering the phosphorus removed with the addition of the precipitated ferric chloride, the ratio between the added Fe and the eliminated phosphorus (Fe/P) varied between 7.2 and 20.3 mol Fe/mol P.

The added iron dose range is higher than the typical values used to eliminate phosphorus in urban wastewater by chemical precipitation. De Gregorio et al. [29] studied the phosphates precipitation in an activated sludge process using ferric chloride, establishing three ranges expressed in mol Fe/mol P: high (1.9–2.3), medium (1.5–1.9) and low (1.0–1.4). However, the iron doses used are the same order of magnitude as the doses needed to obtain low concentrations of phosphorus in urban WWTP. Bratby [30] describes several studies where ferric chloride was used to obtain phosphorus concentrations in the effluent lower than 0.12 mg P L^{-1} in urban WWTP. In these cases, doses between 3.4 and 31.4 mg Fe L^{-1} and molar ratios between 2.5 and 81 mol Fe/mol P were used.

Fig. 3 shows the effect of the addition of precipitated ferric chloride in the increment of non-volatile suspended solids, the flocs density and dry sludge density. Fig. 3a, evidence that the Δ_nVSS linearly increased with the dose (Δ_nVSS = nVSSprec ·d) as it was expected since the precipitate is formed by iron hydroxides, and thus, all the added solids are nVSS. The slope of the nVSS linear increment (nVSSprec) has its value between 36.2 and 39.9 g L^{-1} in the four sludge samples. The variable nVSSprec represents the SS concentration of the precipitate incorporated into the activated sludge flocs. The nVSSprec concentration is greater than the added Fe concentration (24 g Fe L^{-1}) since the precipitated is formed by iron hydroxides.

It can be seen in Fig. 3b and c that both densities vary linearly with the dose of precipitated ferric chloride, being possible to obtain a relationship that allows calculating the density according to the dose of precipitated added. The results agree with those of Jones and Schuler [31], who evidenced that the density of the activated sludge flocs increases linearly with its content in non-volatile suspended solids. The

Table 2
Analytical results of suspended solids, non-volatile suspended solids, floc density and dry sludge density in each test.

Sludge sample	Test number	d [mL L^{-1}]	SS [g L^{-1}]	ε_SS [g L^{-1}]	nVSS [g L^{-1}]	ε_nVSS [g L^{-1}]	Δ_nVSS [g L^{-1}]	ρ_f [g mL^{-1}]	ε_ρ_f [g mL^{-1}]	ρ_s [g mL^{-1}]	ε_ρ_s [g mL^{-1}]
S1	1	0.00	2.26	0.09	0.30	0.02	0.00	1.0355	0.002	1.516	0.002
	2	2.50	2.39	0.09	0.43	0.02	0.13	1.0374	0.002	1.579	0.005
	3	10.0	2.61	0.10	0.63	0.03	0.33	1.0404	0.002	1.656	0.007
	4	15.0	2.83	0.10	0.87	0.04	0.58	1.0457	0.002	1.785	0.013
S2	5	0.00	2.02	0.08	0.28	0.02	0.00	1.0335	0.002	1.543	0.005
	6	1.25	2.05	0.08	0.33	0.02	0.05	1.0357	0.002	1.565	0.004
	7	6.25	2.28	0.09	0.52	0.03	0.24	1.0391	0.002	1.638	0.001
	8	8.50	2.37	0.09	0.63	0.03	0.35	1.0423	0.002	1.659	0.009
S3	9	0.00	3.05	0.11	0.47	0.03	0.00	1.0348	0.002	1.509	0.009
	10	2.50	3.09	0.11	0.56	0.03	0.08	1.0374	0.002	1.567	0.001
	11	5.00	3.16	0.12	0.66	0.03	0.18	1.0391	0.002	1.605	0.004
	12	10.0	3.34	0.12	0.78	0.04	0.30	1.0415	0.002	1.672	0.035
	13	15.0	3.60	0.13	1.05	0.05	0.57	1.0446	0.002	1.674	0.005
S4	14	0.00	2.69	0.06	0.42	0.01	0.00	1.0348	0.002	1.527	0.012
	15	2.50	2.88	0.06	0.56	0.02	0.14	1.0362	0.002	1.564	0.025
	16	5.00	3.04	0.07	0.69	0.02	0.27	1.0401	0.002	1.630	0.003
	17	10.0	3.13	0.07	0.81	0.02	0.39	1.0421	0.002	1.715	0.011
	18	12.5	3.14	0.07	0.83	0.02	0.41	1.0439	0.002	1.709	0.002
	19	15.0	3.40	0.07	1.07	0.03	0.65	1.0473	0.002	1.729	0.008

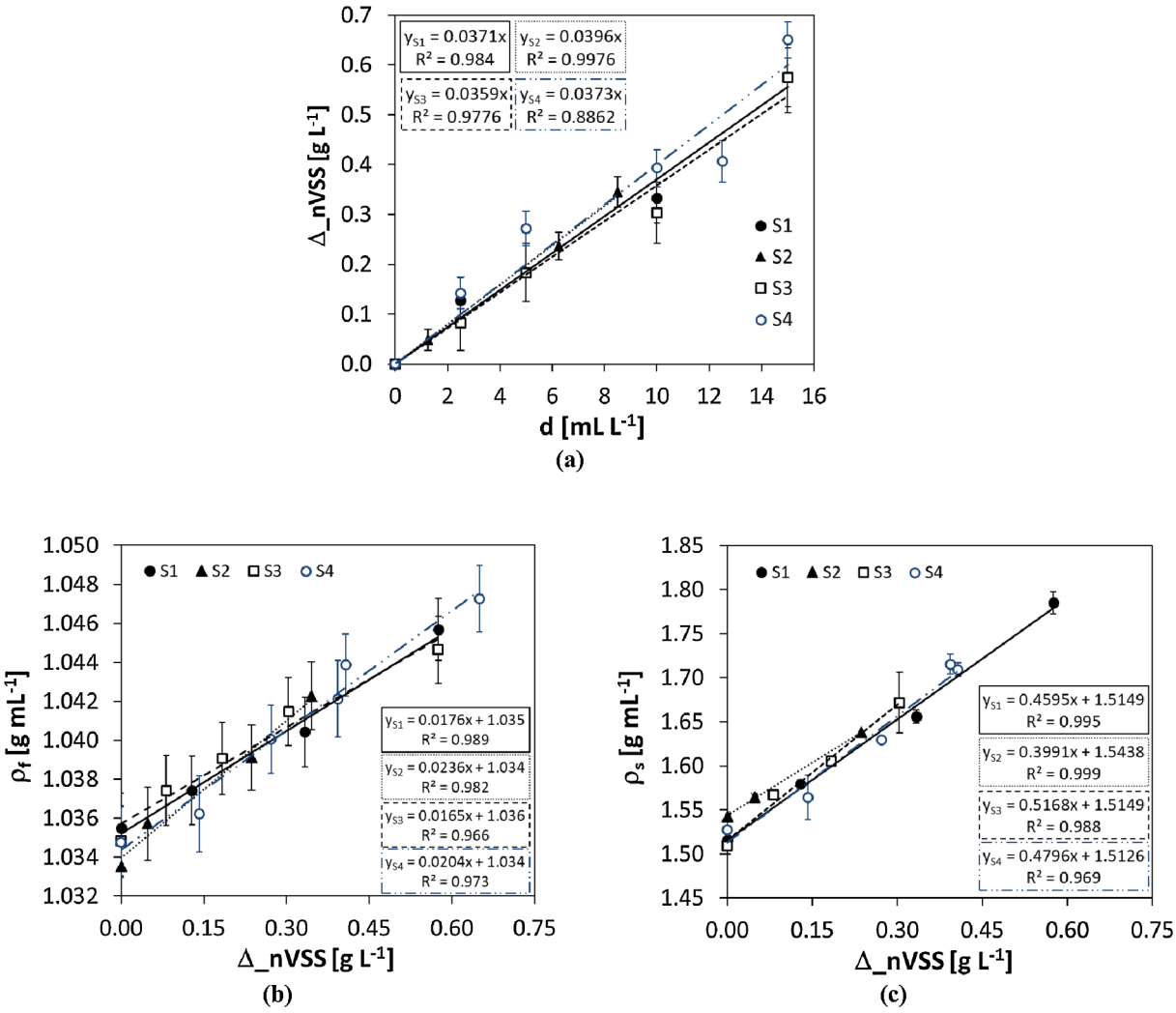

Fig. 3. Influence of the added precipitate on: (a) the increment of non-volatile suspended solids, (b) the flocs density and (c) the dry sludge density.

linear increase of the flocs density is due to the incorporation of precipitated ferric chloride within the flocs. Note that this material, the precipitated coagulant, has a noticeably higher density than the activated sludge flocs (1.035 g mL^{-1} vs 2.54 g mL^{-1}). The dry sludge density is similar to the typical values for urban wastewater treatment plants, which is around 1.45 g mL^{-1} [32]. The floc density measurements are also coherent with the results of Jang and Schuler [28], which ranged from 1.031 to 1.050 g mL^{-1} for activated sludge flocs.

As shown in Fig. 3, slight differences in the nVSS increment as well as in the densities when no precipitate was added were found. They were due to differences in the sludge characteristics, since the samples were collected in four different days and in a period of time in which no changes were observed in the treatment plant operation. However, the linear increase of the nVSS and densities is similar in all cases, since they do not depend on the initial concentration of suspended solids. The results obtained evidence this fact as all the regression are quite similar and even that all data could be fitted to just one regression. On the contrary, the hindered settling velocity depend on the suspended solids concentration, and for this reason, four different sludge samples (with different initial SS concentration) were used, to study this dependency as well as the influence of other relevant parameters like the dose, densities, size and morphology.

3.2. Debris elimination

Microscopic observation of sludge revealed the presence not only of sludge flocs and protist populations, but also debris, which can include small inert particles present in the sludge, free precipitated coagulant particles, and so on. These small aggregates should not be considered in the size and morphological characterization of the sludge flocs since they would alter the results of the quantitative analysis. This is especially important in cases where small flocs predominate, like activated sludge with “pin-point floc” structure typical in extended aeration biological processes where flocs are characterized by being weak and easily breakable. A recent research by Asensi *et al.* [23] found that almost 85% of the flocs from the biological reactor of Ford-Almussafes WWTP (Valencia, Spain) had small size with an equivalent diameter smaller than 25 μm.

Usually, the debris is eliminated by deleting all objects smaller than a fixed area [25]. However, visual inspection of many of the collected images revealed that in the small size range (0 – 25 μm) both populations, debris and flocs, were mixed. For this reason, a more elaborated methodology based on size distribution and morphological parameters was devised to discriminate between both populations.

Among the parameters determined in the morphological study, two were of special importance for a precise and objective discrimination of the debris from the small activated sludge flocs. These parameters were: aspect ratio and floc size distribution.

The aspect ratio (AR) indicates the relationship between the length and width of an object. This parameter contributes to differentiate between the elongated flocs and the small spherical particles of debris. Fig. 4a shows the AR values for the five tests performed with the sludge

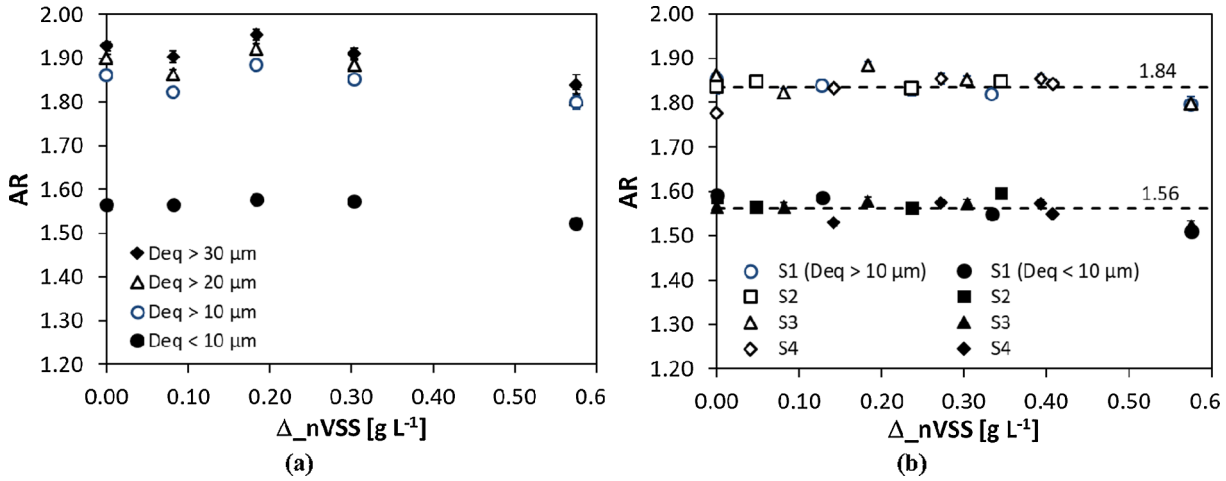

Fig. 4. Aspect ratio for: (a) four size ranges (D_{eq} < 10, > 10, > 20 and > 30 µm) of the particles from sludge sample S3, (b) the floc (D_{eq} > 10 µm) and debris (D_{eq} < 10 µm) populations from all samples.

sample S3 (Table 1), calculated considering the following size ranges of the objects: 0–10 µm, higher than 10 µm, higher than 20 µm and higher than 30 µm. In this figure, it can be observed that the AR parameter, for those objects with equivalent diameter (D_{eq}) > 10 µm, took values around 1.9 and higher (no matter the quantity of precipitated ferric chloride added). However, considering only the objects between 0 and 10 µm, the resulting values of AR were lower (around 1.56), indicating objects that have a very different form (less elongated) than the rest of the population. In the elaboration of the figure, the amount of precipitate ($FeCl_3$) added has been explicitly considered. The Krustal-Wallis test confirmed that the group of objects with Deq lower than 10 µm was statistically different from the other. Fig. 4b confirms that the AR of the debris (particles with Deq < 10 µm) is clearly lower than the AR of the floc population (Deq > 10 µm) for all samples.

The size distribution is especially important in the debris study. Fig. 5 shows the size distribution for the population of particles with equivalent diameter between 0 and 10 µm.

In this figure it can be observed that the size of the particles follow a lognormal distribution with average value close to 7 µm. In the left part of the distribution, there are no sizes smaller than 4.5 µm due to the elimination of noise during the pre-processing of the images. In the right part of the distribution, the presence of spikes can be attributed to the coexistence of both populations, debris and flocs.

Through this morphological analysis it was concluded that populations with sizes between 0 and 10 µm and sizes > 10 µm were geometrically different. Therefore, for the studied activated sludge, a value of 10 µm expressed as equivalent diameter was established as debris.

3.3. Floc size

Several calculated parameters reflect the size of the sludge flocs: area, equivalent diameter, length and radius of gyration. The equivalent diameter is closely related to the length and the radius of gyration (as Fig. 6 shows), and it is calculated from the area. Therefore, only D_{eq} results are shown and discussed.

It was observed that the equivalent diameter of flocs coming from the original sludge, and from sludge with a small or moderate dose of added precipitate, followed a lognormal distribution. The equivalent diameter distribution was not lognormal for high doses of precipitate (15 mL $FeCl_3$). Therefore, the median of the equivalent diameter can be considered the most representative parameter of the floc size distribution.

In the activated sludge under study, a debris population formed by objects with a Deq < 10 µm and a flocs population were identified. The flocs population was classified in three groups according to their equivalent diameter: small (Deq < 25 µm), intermediate (25 µm < Deq < 250 µm) and large (Deq > 250 µm) flocs. The flocs percentage with respect to the total number of flocs (%Nb) was calculated in each group as well as the percentage of area in each group with respect to the total area of the flocs (%Area). Mezquita et al. [33] used this classification of flocs to study the sedimentability of the activated sludge and Mezquita et al. [34] used it to estimate the effluent quality of an activated sludge process.

Fig. 7 shows the effect of the precipitate addition on %Nb and %Area in each size group. In the tests carried out without the addition of precipitate, it was observed that the small (46.8–51.7%) and intermediate (45.8–51.9%) flocs predominated with a similar percentage, while the percentage of large flocs was very small (0.5–2.5%). However, the %Area of the small flocs group was very small (1.9–3.7%), showing the intermediate flocs a %Area (52–84.1%) greater than the large ones (12.3–46.1%).

The addition of precipitate changed the proportion of flocs in the different size groups. An increase in the precipitate dose led to the linear decrease of the intermediate %Nb, and the linear increase of the small and large %Nb (Fig. 7). The slopes obtained in the linear fits performed show that the decrease of the intermediate %Nb generates a larger proportion of large flocs than small flocs. The changes in the %Nb are due to the flocs fragmentation processes that can occur during the rapid mixing phase and to the aggregation processes during the slow agitation phase favoured by the presence of the precipitated coagulant. The decrease of the intermediate %Nb and the increase of the large %Nb with the precipitate addition led to the decrease of the intermediate %Area and to the increase of the large %Area. However, the small %Area decreased due to the increase in the number and size of large flocs when the precipitate is added.

Although the size of the total flocs population, described by the median of the Deq, decreased slightly with the addition of the precipitate, the mean of the Deq increased linearly (see Fig. 8 a and b) as a consequence of the increase of the large flocs %Nb and %Area. This floc size variation, together with the increase in density due to the incorporation to the floc structure of a higher density precipitate (around 2.54 g mL^{-1}) than the sludge flocs (around 1.035 g mL^{-1}), will significantly impact the hindered settling velocity. Research literature relating floc size to coagulant dose in activated sludge shows a variety of results. Some authors reported a positive relationship. For example, Chen and Wang [35] concluded that activated sludge flocs' size increased with the addition of the polymeric ferric sulfate. Other authors, like Caravelli *et al.* [36] found a reduction in the activated sludge flocs' size with the addition of ferric chloride.

No clear pattern was observed explaining the variability of the shape factors with the added precipitate. However, the relationship

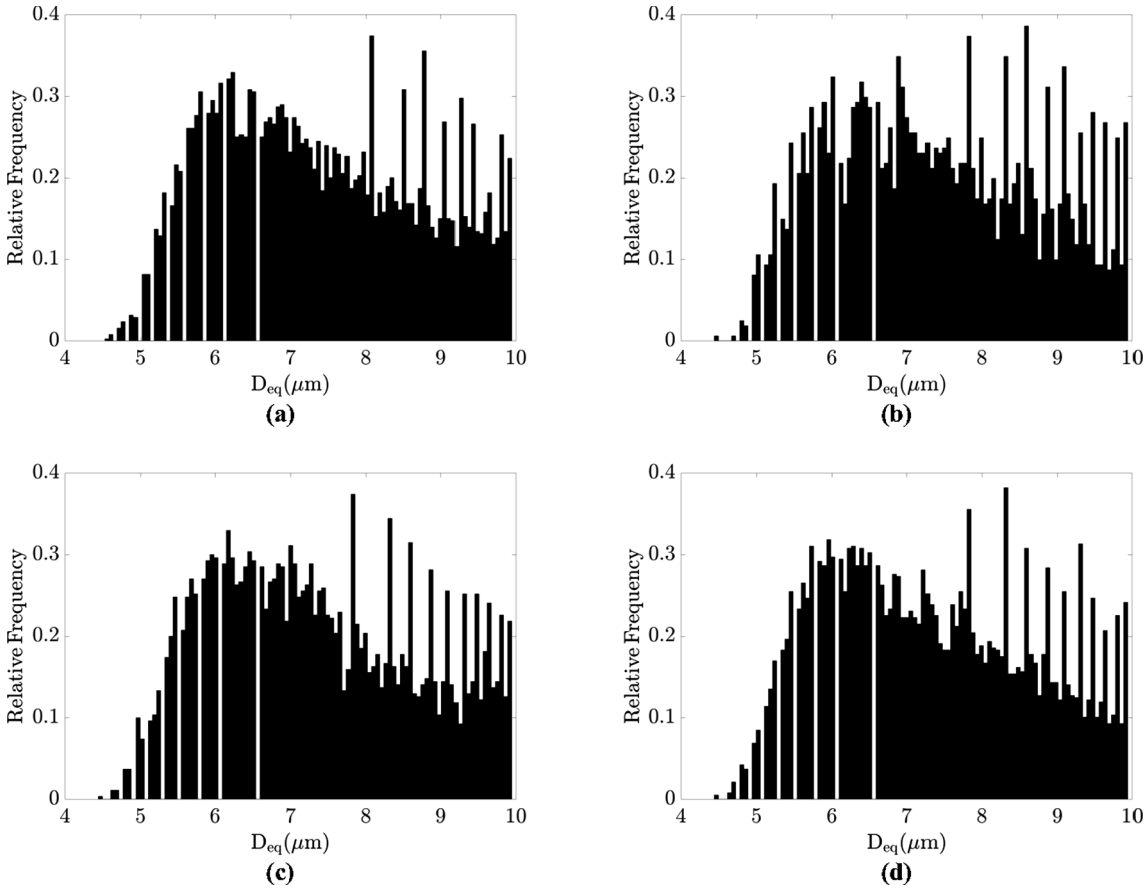

Fig. 5. Size distributions from 0 to 10 µm from a test performed on sludge sample: (a) S1, (b) S2, (c) S3 and (d) S4.

between the form factor (FF) and the size of flocs, shown in Fig. 8c, is interesting. That is, the larger the size of the flocs in the original activated sludge samples the lower the form factor. This relationship was also observed in all the tests carried out after adding ferric chloride precipitate. The fractal dimension $Df_{A\text{-}P}$ relates area to flocs perimeter by $A \sim P^{2/Dfa\text{-}p}$, so that $P \sim A^{Dfa\text{-}p/2}$. Substituting this expression into the FF definition ($FF = 4\pi \cdot A/P^2$) and considering that $A = D_{eq}^{\ 2}\ \pi/4$, gives $FF \sim D_{eq}^{\ 2\cdot(1\text{-}Dfa\text{-}p)}$. Thus, the experimental results in Fig. 8c can be explained from the fractal structure of the flocs, since given that $Df_{A\text{-}P} > 1$ (Fig. 9b), then $(1\text{-}Df_{P\text{-}A}) < 0$ and $FF \sim D_{eq}^{\ -\alpha}$. These results mean that larger flocs are more irregular and have shapes of longer perimeter.

3.4. Fractal dimension

Fig. 9 shows the two-dimensional fractal dimensions calculated to assess and quantify changes in the irregularities of the sludge flocs structure due to the addition of the ferric chloride precipitate. As shown in Fig. 9a, the fractal dimension obtained from the area and length of the flocs ($Df_{A\text{-}L}$) increases with the added dose of precipitate. The increment in this fractal dimension indicates that the addition of precipitate leads to a more compact floc structure, with larger area. In almost all the tests, the increment seems to be linear with respect to the increment in the precipitate's dose. Chen and Wang [35] also found that the $Df_{A\text{-}L}$ of activated sludge rapidly increased with an increase in

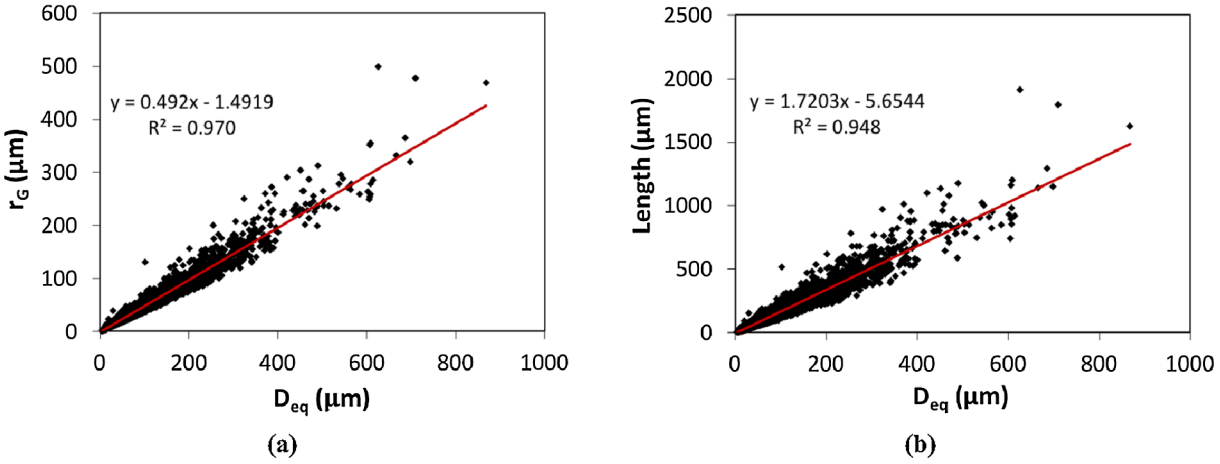

Fig. 6. Relationship between size factors: (a) equivalent diameter versus radius of gyration (b) equivalent diameter versus length.

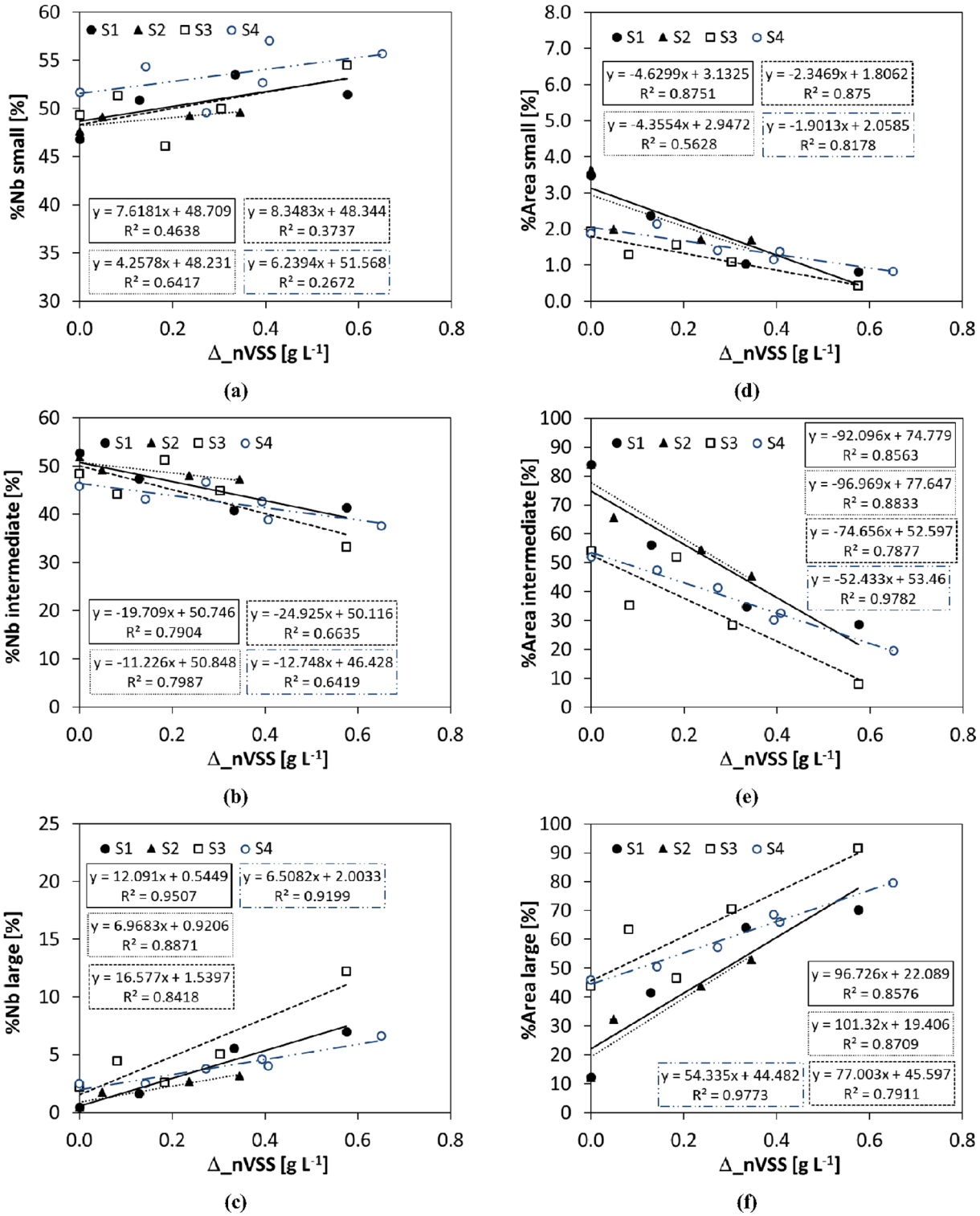

Fig. 7. Influence of the added precipitate on the flocs number percentage (%Nb) and on the flocs area percentage (%Area) for small, medium and large flocs: (a) %Nb small, (b) %Nb intermediate, (c) %Nb large, (d) %Area small, (e) %Area intermediate, (f) %Area large.

polymeric ferric sulfate dosages at low values of the flocculant dosage.

Fig. 8b shows how the fractal dimension obtained from the area and the perimeter of flocs ($Df_{A\text{-}P}$) decreases at high doses of ferric chloride precipitate. This decrement indicates that the sludge flocs coming from sludge with no added precipitate have shorter perimeter. Therefore, the structure of the flocs is more closed, with more regular edges. It is also observed, that such decrease fits better to a polynomial function than to a regression line.

The fractal dimensions were clearly influenced by the addition of the precipitated reagent. The addition of the precipitate and the subsequent flocculation process produced flocs with larger area but less perimeter, that is, more compact, closed and regular flocs.

3.5. Settling velocity

Fig. 10 demonstrates the impact of the addition of ferric chloride

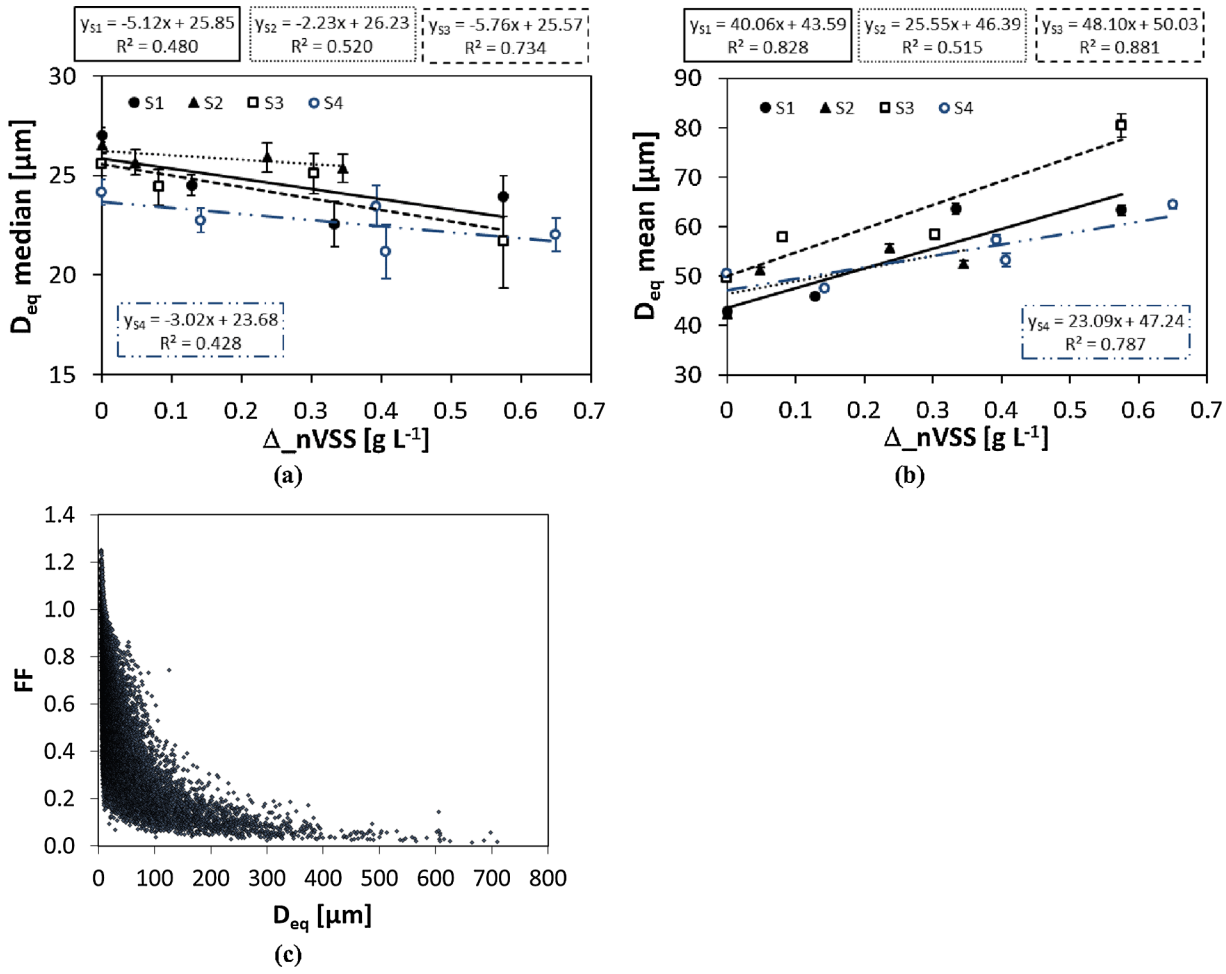

Fig. 8. Influence of the precipitated ferric chloride on the size of flocs: (a) Deq median and (b) Deq mean. (c) Variation of the form factor with the size of flocs in the original activated sludge samples (that is, with no added precipitate).

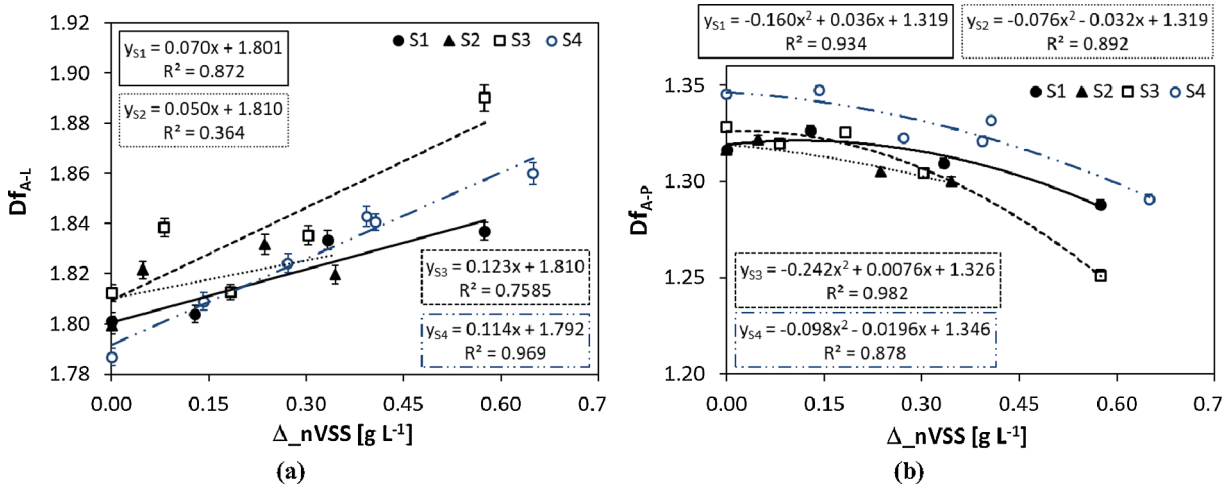

Fig. 9. Influence of the addition of ferric chloride precipitate on the fractal dimension obtained from: (a) the area and the length of the sludge flocs $Df_{A\text{-}L}$ (b) the area and the perimeter of the sludge flocs $Df_{A\text{-}P}$.

precipitate on the hindered settling velocity of the activated sludge. To visualize better this impact, the sedimentation velocity was expressed as $Vs\text{-}Vs_i$, Vs_i being the settling velocity of the sludge with no added precipitate. This figure shows that the hindered sedimentation velocity varies linearly with the increment in the dose of precipitate. In other studies, it was also found an increase in the hindered settling velocity with the nVSS concentration. Vanderhasselt and Verstraete [3] showed that settling velocity increased with the addition of talc, increase that was linear in the case of the activated sludge of an industrial wastewater treatment plant. Jones and Schuler [17] showed that an increase of nVSS in the activated sludge causes an increment in the density of the flocs, and that the increment of density improves the sedimentability of the sludge.

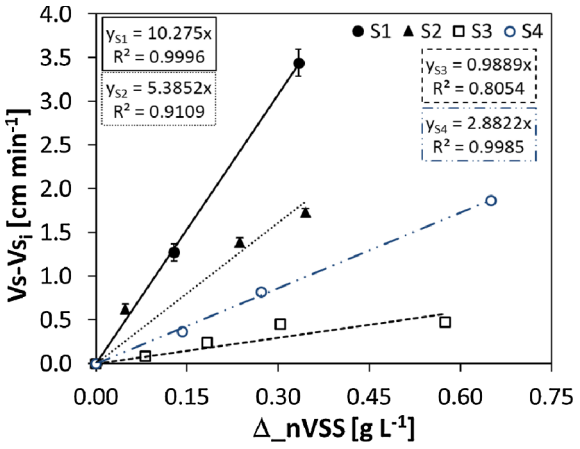

Fig. 10. Variation of the sedimentation velocity with the dose of precipitate.

The obtained results evidence that the addition of the $FeCl_3$ precipitate is a feasible and interesting option to improve the performance and removal of suspended solids of the secondary settler thanks to the improvement in the hindered settling velocity. This low-cost option for short periods (like disturbances or emergency situations) can help the WWTP to meet the effluent discharge legal requirements. Not only phosphorus contained in the suspended solids would be removed but also, through absorption, part of the soluble phosphorus. The phosphates elimination by precipitate addition have been explained by surface complexation processes and phosphorus adsorption [7,8]. Zhao et al. [9] also showed the efficiency of granular ferric hydroxide to remove phosphates by adsorption.

Finally, multivariate statistical projection methods were used to find which variables (density, size, fractal dimensions and morphological parameters of the flocs) were more related to the hindered settling velocity of the activated sludge. Different researches [34,37] have highlighted the usefulness of chemometric methods in combination with image analysis for process monitoring and interpretation in activated sludge wastewater treatment systems.

First, principal component analysis (PCA) was conducted on the preprocessed data (mean-centered and scaled to unit variance) to get a graphical overview of the relationship among all the variables. The data matrix analysed was formed by the values of the 17 variables (including the settling velocity) in the 19 tests. To characterize the size and morphology of the flocs population the median was considered due to the asymmetry of the data that followed a lognormal distribution (no distinction between size groups was made). Four principal components were statistically significant according to cross-validation, explaining 55.8%, 18.7%, 13.7% and 6.88% of the total variance, respectively. The main results of the analysis are displayed in Fig. 11. As can be seen in the first two components score-plot (Fig. 11a), the four test samples (T1, T5, T9 and T14) with no precipitate added (each test corresponds to a different sludge sample: S1 to S4) were projected on the lower-left quadrant. As the dose of ferric chloride precipitate was increased, the corresponding test sample projection tends to move up and to the right. A clear trajectory can be seen following the projection of all the tests of each sludge sample (S1 to S4) in this score-plot (e.g., T14 to T19 for sludge sample S4). To facilitate the visualization of these trajectories, a different symbol was used for each sludge sample. These trajectories are coherent with the loading plot of these first two components (Fig. 11c). Recall that this loading plot exhibited relevant and clear positive correlations between density, nVSS and precipitated coagulant added, variables which are located on the upper-right quadrant of the plot. Therefore, as the amount of precipitated coagulant added is increased, the test projection tends to move in that direction. The score-plot of third and fourth components (Fig. 11b), reflected the greatest separation between the sludge samples (S1 to S4), being almost all tests from the same sludge sample in the same quadrant.

The loading plots (Fig. 11c and d) show the relationships among the variables: positively correlated variables are close in the plot, while negatively correlated variables are in opposite quadrants. In Fig. 11c, clear positive correlations can be observed between the following groups of variables: density, nVSS and precipitated coagulant added; equivalent diameter, length and perimeter; aspect ratio and radius of gyration; form factor and roundness. In these two principal component loading plots, the form factor and radius of gyration are negatively correlated, while in Fig. 11d, the hindered settling velocity appear negatively correlated with three variables: volumetric fraction of the sludge (Fv), SS and the fractal dimension that relates area – perimeter ($Df_{A\text{-}P}$).

Partial Least Square (PLS) regression was used to develop a model to predict the hindered settling velocity (y-variable) from the rest of the variables (X-variables). This multivariate projection method seeks to maximize the covariance between both X and Y. The application of this technique to biomass morphological and physiological data has allowed reasonably prediction of key effluent parameters, COD, N-NH_4^+ and N-NO_3^- [34] and sludge settling properties [33]. Therefore, these data could provide relevant information to estimate key parameters of the activated sludge process and the PLS be a suitable method to discover it.

The PLS model developed using all the data from the 19 tests, resulted in two statistically significant variables. The model exhibited a good balance between fit and prediction performance, with an explained variation parameter of 67.9% (R^2x), 85.1% (R^2y) and a goodness of prediction parameter (Q^2) of 77.1%. Fig. 12a, shows the importance of each X-variable on the predictive model developed. As shown in the figure, the variables with most predictive capability (i.e., variables more related to Vs) are the volumetric fraction of the sludge (Fv), SS and the fractal dimension that relates area – perimeter ($Df_{A\text{-}P}$). In hindered settling, it is expected a decrease of the settling velocity as the concentration of solids increases. The volumetric fraction of the sludge is calculated from the dry sludge density and the solid concentration. Therefore, these two variables could be expected to be well correlated with the hindered settling velocity. However, it was interesting to find that a fractal dimension was more correlated with the velocity than the density and size of the flocs, which are the parameters that determine the settling velocity in the free-settling of the particles (Type I). This result is coherent with the research of Piirtola *et al.* [4] who concluded that differences in density and particle size, or the concentration of soluble cations do not explain the effect of mineral materials on the activated sludge settleability.

Fig. 12b shows the performance of the PLS model developed with the 19 tests using the 16 measured variables (size, fractal dimensions and morphological parameters of the flocs) to predict the hindered settling velocity. As the figure shows, model performance is reasonable considering that the model was developed with the whole set of data (19 tests) and thus, included four different sludge samples (S1 to S4). Clearly, a better fit could be achieved if four PLS models were developed: a model for each sludge sample (similarly to Fig. 10, where a regression model was developed using all the tests for each sludge sample).

4. Conclusions

In this work, interesting experimental results on the effect of the addition of a ferric chloride precipitate on the morphological characteristics of the sludge flocs and on the hindered settling velocity are presented and thoroughly analysed and discussed. These results were obtained using quantitative image analysis techniques. The main conclusions that can be drawn from this study are:

- The density of both, flocs and dry sludge, vary linearly with the dose of ferric chloride precipitate.
- A clear (and close to linear) increment in the mean equivalent

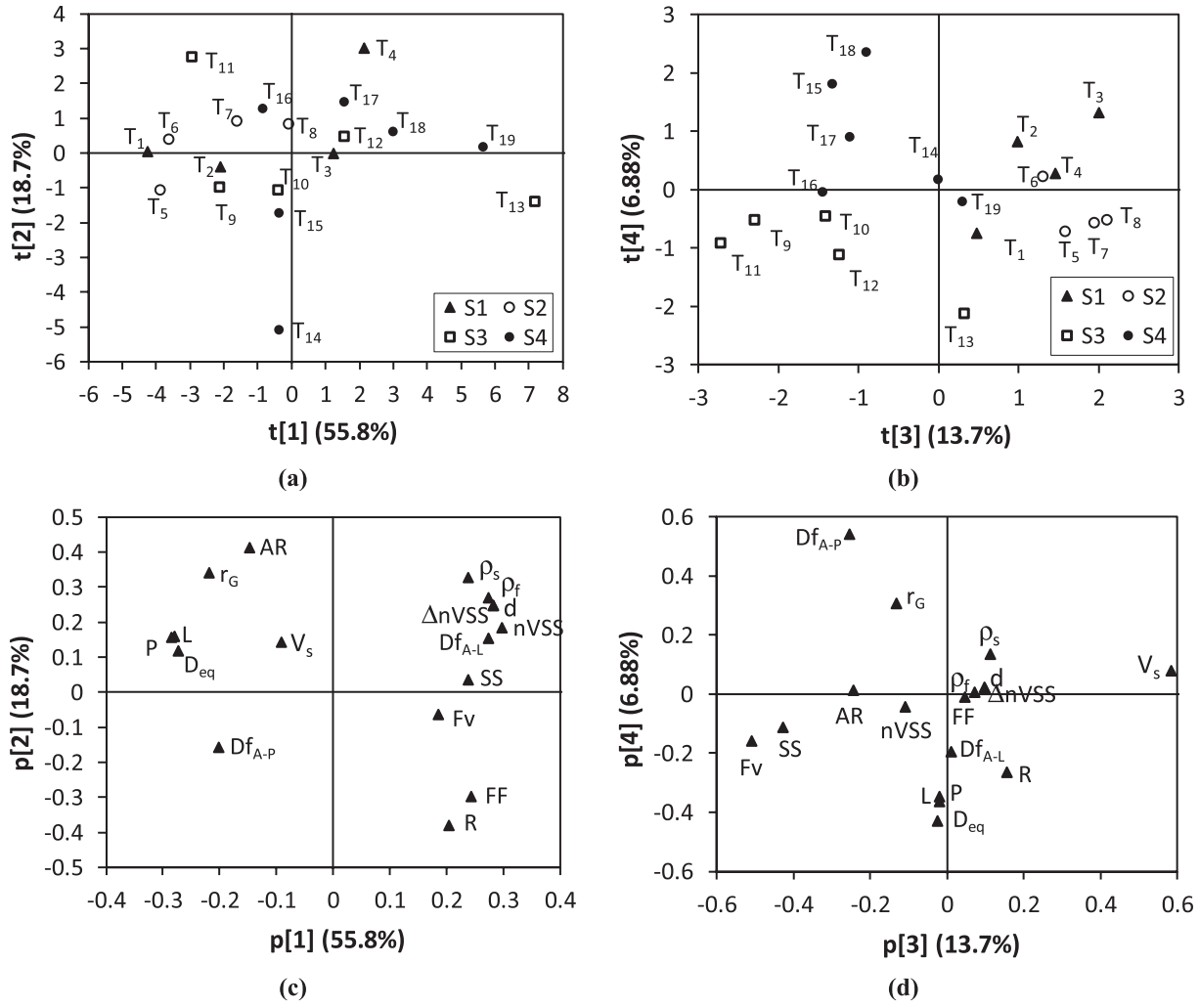

Fig. 11. Score plots (a and b) and loading plots (c and d) of the four component PCA model (explaining 95.08% of the variance) fitted to the 19 tests. Variables included: aspect ratio (AR), radius of gyration (r_G), hindered settling velocity (Vs), perimeter (P), Length (L), equivalent diameter (D_{eq}), dose of ferric chloride precipitate (d), volumetric fraction of the sludge (Fv), fractal dimension that relates area – perimeter (Df_{A-P}), fractal dimension that relates area – length (Df_{A-L}), roundness (R), total suspended solids (SS), non-volatile suspended solids (nVSS), dry sludge density (ρ_s), flocs density (ρ_f), increment of non-volatile suspended solids (Δ _nVSS) with respect to the concentration of nVSS in the test with no added precipitate (i.e., Δ _nVSS = [nVSS – $nVSS_i$]).

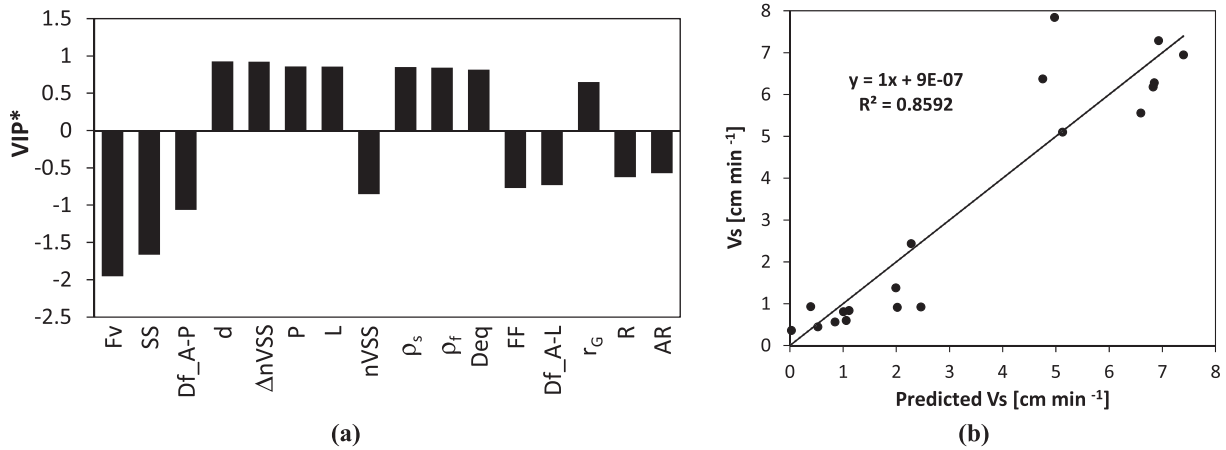

Fig. 12. PLS developed with all the tests: (a) Importance of each variable on the predictive model multiplied by its correlation sign to enable visualization of positive and negative dependencies with the settling velocity (b) Measured values of the hindered settling velocity versus PLS predicted values. Predicted values are based on the size, fractal dimensions and morphological parameters of the flocs.

diameter of the sludge flocs related to the increase of the added dose of precipitate was observed.

- A new methodology based on geometric arguments is proposed to discriminate the debris from small activated sludge flocs. Two morphological parameters: aspect ratio and floc size distribution, allowed a precise and objective discrimination.
- Variations in the fractal dimensions obtained from the area, perimeter and length of the flocs indicate that the addition of precipitate and the subsequent flocculation process led to flocs with more area and less perimeter, that is, more compact, closed and regular flocs.
- The hindered settling velocity of the activated sludge linearly increases with the addition of ferric chloride precipitate. This is due to an increment in the sludge density as a result of the incorporation of the precipitate into the activated sludge floc structure.
- Multivariate data analysis showed that the most related variables to the hindered settling velocity were the volumetric fraction of the sludge (Fv), the SS concentration and the fractal dimension that relates area – perimeter ($Df_{A\text{-}P}$).

Acknowledgements

This research work did not receive any specific grant from funding agencies in the public, commercial, or not-for-profit sectors.

References

[1] E. Metcalf, H. Eddy, Wastewater engineering: treatment and reuse, 2003. http://doi.org/10.1007/s13398-014-0173-7.2.
[2] C.P.L. Grady Jr, G.T. Daigger, N.G. Love, C.D.M. Filipe, others, Biological wastewater treatment, IWA Publishing, 2011.
[3] A. Vanderhasselt, W. Verstraete, Short-term effects of additives on sludge sedimentation characteristics, Water Res. 33 (1999) 381–390, https://doi.org/10.1016/S0043-1354(98)00204-8.
[4] L. Piirtola, R. Uusitalo, A. Vesilind, Effect of mineral materials and cations on activated and alum sludge settling, Water Res. 34 (1999) 191–195, https://doi.org/10.1016/S0043-1354(99)00134-7.
[5] J. Wiszniowski, J. Surmacz-Górska, D. Robert, J.V. Weber, The effect of landfill leachate composition on organics and nitrogen removal in an activated sludge system with bentonite additive, J. Environ. Manage. 85 (2007) 59–68, https://doi.org/10.1016/j.jenvman.2006.08.001.
[6] M. Lapointe, B. Barbeau, Characterization of ballasted flocs in water treatment using microscopy, Water Res. 90 (2016) 119–127, https://doi.org/10.1016/j.watres.2015.12.018.
[7] S. Smith, I. Takács, S. Murthy, G.T. Daigger, A. Szabó, Phosphate complexation model and its implications for chemical phosphorus removal, Water Environ. Res. 80 (2008) 428–438, https://doi.org/10.1002/j.1554-7531.2008.tb00349.x.
[8] I. Takács, B.R. Johnson, S. Smith, A. Szabó, S. Murthy, P. Chemical, removal – from lab tests through model understanding to full-scale demonstration, IWA Spec. Conf. Des. Oper. Econ. Large Watstewater Treat. Plants. (2011) 101–108.
[9] B. Zhao, Y. Zhang, X. Dou, H. Yuan, M. Yang, Granular ferric hydroxide adsorbent for phosphate removal: Demonstration preparation and field study, Water Sci. Technol. 72 (2015) 2179–2186, https://doi.org/10.2166/wst.2015.438.
[10] K. Grijspeerdt, W. Verstraete, Image analysis to estimate the settleability and concentration of activated sludge, Water Res. 31 (1997) 1126–1134, https://doi.org/10.1016/S0043-1354(96)00350-8.
[11] B. Jin, B.M. Wilén, P. Lant, A comprehensive insight into floc characteristics and their impact on compressibility and settleability of activated sludge, Chem. Eng. J. 95 (2003) 221–234, https://doi.org/10.1016/S1385-8947(03)00108-6.
[12] B.M. Wilén, D. Lumley, A. Mattsson, T. Mino, Relationship between floc composition and flocculation and settling properties studied at a full scale activated sludge plant, Water Res. 42 (2008) 4404–4418, https://doi.org/10.1016/j.watres.2008.07.033.
[13] E. Koivuranta, J. Keskitalo, T. Stoor, J. Hattuniemi, M. Sarén, J. Niinimäki, A comparison between floc morphology and the effluent clarity at a full-scale activated sludge plant using optical monitoring, Environ. Technol. (United Kingdom) 35 (2014) 1605–1610, https://doi.org/10.1080/09593330.2013.875065.
[14] E. Liwarska-Bizukojc, M. Bizukojc, The influence of the selected nonionic surfactants on the activated sludge morphology and kinetics of the organic matter removal in the flow system, Enzyme Microb. Technol. 41 (2007) 26–34, https://doi.org/10.1016/j.enzmictec.2006.11.016.
[15] D.P. Mesquita, A.L. Amaral, E.C. Ferreira, Characterization of activated sludge abnormalities by image analysis and chemometric techniques, Anal. Chim. Acta. 705 (2011) 235–242, https://doi.org/10.1016/j.aca.2011.05.050.
[16] E. Liwarska-Bizukojc, A. Klepacz-Smółka, O. Andrzejczak, Variations of morphology of activated sludge flocs studied at full-scale wastewater treatment plants, Environ. Technol. (United Kingdom) 36 (2015) 1123–1131, https://doi.org/10.1080/09593330.2014.982717.
[17] Patricia A. Jones, Andrew J. Schuler, Role of changing biomass density in process disruptions affecting biomass settling at a full-scale domestic wastewater treatment plant, J. Environ. Eng. 138 (1) (2012) 67–73, https://doi.org/10.1061/(ASCE)EE.1943-7870.0000468.
[18] J.C. Costa, D.P. Mesquita, A.L. Amaral, M.M. Alves, E.C. Ferreira, Quantitative image analysis for the characterization of microbial aggregates in biological wastewater treatment: A review, Environ. Sci. Pollut. Res. 20 (2013) 5887–5912, https://doi.org/10.1007/s11356-013-1824-5.
[19] D.P. Mesquita, A.L. Amaral, E.C. Ferreira, Activated sludge characterization through microscopy: A review on quantitative image analysis and chemometric techniques, Anal. Chim. Acta. 802 (2013) 14–28, https://doi.org/10.1016/j.aca.2013.09.016.
[20] M.S. Nasser, Characterization of floc size and effective floc density of industrial papermaking suspensions, Sep. Purif. Technol. 122 (2014) 495–505, https://doi.org/10.1016/j.seppur.2013.12.008.
[21] B. Wang, Y. Shui, M. He, P. Liu, Comparison of flocs characteristics using before and after composite coagulants under different coagulation mechanisms, Biochem. Eng. J. 121 (2017) 107–117, https://doi.org/10.1016/j.bej.2017.01.020.
[22] G.W. Chen, I.L. Chang, W.T. Hung, D.J. Lee, Regimes for zone settling of waste activated sludges, Water Res. 30 (1996) 1844–1850, https://doi.org/10.1016/0043-1354(95)00322-3.
[23] E. Asensi, E. Alemany, A. Seco, J. Ferrer, Characterization of activated sludge settling properties with a sludge collapse-acceleration stage, Sep. Purif. Technol. 209 (2019) 32–41, https://doi.org/10.1016/j.seppur.2018.07.006.
[24] P. François, F. Locatelli, J. Laurent, K. Bekkour, Experimental study of activated sludge batch settling velocity profile, Flow Meas. Instrum. 48 (2016) 112–117, https://doi.org/10.1016/J.FLOWMEASINST.2015.08.009.
[25] D.P. Mesquita, O. Dias, A.L. Amaral, E.C. Ferreira, A comparison between bright field and phase-contrast image analysis techniques in activated sludge morphological characterization, Microsc. Microanal. 16 (2010) 166–174, https://doi.org/10.1017/S1431927609991358.
[26] American Public Health Association, American Water Works Association, Water Environment Federation, Standard Methods for the Examination of Water and Wastewater. 22nd ed., Am. Public Heal. Assoc. Washingto, DC, USA. (2012). doi:ISBN 9780875532356.
[27] I. Nopens, Modelling the activated sludge flocculation process : a population balance approach, 2005. https://rolland.ugent.be/catalog/rug01:000894656%0A http://lib.ugent.be/fulltxt/RUG01/000/894/656/RUG01-000894656_2010_0001_AC.pdf.
[28] H. Jang, A.J. Schuler, The case for variable density: A new perspective on activated sludge settling, Water Environ. Res. 79 (2007) 2298–2303, https://doi.org/10.2175/106143007X194347.
[29] C. De Gregorio, A.H. Caravelli, N.E. Zaritzky, Performance and biological indicators of a laboratory-scale activated sludge reactor with phosphate simultaneous precipitation as affected by ferric chloride addition, Chem. Eng. J. 165 (2010) 607–616, https://doi.org/10.1016/j.cej.2010.10.004.
[30] J. Bratby, Coagulation and flocculation in water and wastewater treatment, Third Ed., IWA Publishing, London, 2016 doi:ISBN 9781780407494.
[31] P.A. Jones, A.J. Schuler, Seasonal variability of biomass density and activated sludge settleability in full-scale wastewater treatment systems, Chem. Eng. J. 164 (2010) 16–22, https://doi.org/10.1016/j.cej.2010.07.061.
[32] G.A. Ekama, J.L. Barnard, F.W. Günthert, P. Krebs, D.S. McCorquodale, J. A. Parker, E.J. Wahlberg, Secondary settling tank: theory, modelling, design and operation. Scientific and Technical Report No. 6. IAWQ, International Association on Water Quality, London, 1997. doi:ISBN 9781900222037.
[33] D.P. Mesquita, O. Dias, A.M.A. Dias, A.L. Amaral, E.C. Ferreira, Correlation between sludge settling ability and image analysis information using partial least squares, Anal. Chim. Acta. 642 (2009) 94–101, https://doi.org/10.1016/j.aca.2009.03.023.
[34] D.P. Mesquita, A.L. Amaral, E.C. Ferreira, Estimation of effluent quality parameters from an activated sludge system using quantitative image analysis, Chem. Eng. J. 285 (2016) 349–357, https://doi.org/10.1016/j.cej.2015.09.110.
[35] Q. Chen, Y. Wang, Influence of single- and dual-flocculant conditioning on the geometric morphology and internal structure of activated sludge, Powder Technol. 270 (2015) 1–9, https://doi.org/10.1016/j.powtec.2014.10.002.
[36] A.H. Caravelli, C. De Gregorio, N.E. Zaritzky, Effect of operating conditions on the chemical phosphorus removal using ferric chloride by evaluating orthophosphate precipitation and sedimentation of formed precipitates in batch and continuous systems, Chem. Eng. J. 209 (2012) 469–477, https://doi.org/10.1016/j.cej.2012.08.039.
[37] A.L. Amaral, D.P. Mesquita, E.C. Ferreira, Automatic identification of activated sludge disturbances and assessment of operational parameters, Chemosphere 91 (2013) 705–710, https://doi.org/10.1016/j.chemosphere.2012.12.066.